International Journal of Engineering Trends and Technology
ISSN: 2231–5381 / https://doi.org/10.14445/22315381/IJETT-V72I8P137

Volume 72 Issue 8, 400-414, August 2024

Original Article

Durability and Microstructure Analyses of Waste Granite Powder for Sustainable Concrete Production

Ahmed Minhajuddin[1], Arijit Saha[2]

[1, 2]*Department of Civil Engineering, GITAM (Deemed to be University), Hyderabad, Telangana, India.*

[2]*Corresponding Author : asaha@gitam.edu*

Received: 25 February 2024 Revised: 18 June 2024 Accepted: 31 July 2024 Published: 28 August 2024

Abstract *- The granite industry produces substantial waste in the form of Waste Granite Powder (WGP) that remains non-biodegradable. This study explores the utilization of WGP in concrete production to have a green solution for waste disposal and environmental problems. Therefore, this study aimed to investigate how replacing fine aggregates with WGP influences both durability and microstructure in concrete. The fresh and hardened WGP blended concrete with different substitution rates of fine aggregate (10% to 50 % by weight) is subjected to durability tests, including water absorption, water penetration, RCPT, and HCP. Further, the microstructural characterization with Scanning Electron Microscopy Energy Dispersive X-ray Spectroscopy (SEM-EDS) and Fourier transform infrared spectroscope analysis is carried out for different WGP blended concrete. The findings indicate that replacing up to 40% fine aggregate with WGP significantly improves concrete's microstructure and durability contrasted to the control mix. This improvement is ascribed to its finer particle size and Si/Al ratio of geopolymers, which encourages better interpore connectivity and geopolymerization. The paper also investigates the relationships among different durability properties. Therefore, the use of WGP in concrete provides a way to solve disposal problems and, at the same time, helps for eco-friendly sustainable construction.*

Keywords *- Fine aggregate, Waste Granite Powder (WGP), Durable Properties, SEM-EDS, FTIR.*

1. Introduction

Around the world, concrete is crucial for enhancing infrastructure and raising the standard of living. To be economically feasible on a large scale, concrete needs to be robust and sustainable, able to withstand extreme weather conditions [1], [2]. Concrete, a key construction material, requires a lot of natural resources, particularly fine aggregate. However, excessive resource extraction of these resources leads to serious environmental problems, necessitating innovative solutions to prevent their depletion [3]. Waste materials can be incorporated into concrete production to help address the challenges of solid waste management. This approach not only reduces costs but also lessens the strain on landfills. Moreover, it addresses the environmental issues related to excessive sand extraction, cement production, and air pollution, contributing to significant benefits to both society and the environment. According to research, various types of solid waste are used in concrete production, such as stone by-products, plastics, agricultural residues, slag, and paper waste [1]. These wastes can serve as cementitious materials [4], fine aggregates [5], coarse aggregates [6], fillers [7], mineral admixtures [8], and pozzolanic materials [9]. Studies illustrate that incorporating these waste materials often results in concrete that performs as well as or even better than traditional mixes. Specifically, concrete comprising silica sand, basalt, marble waste, and granite exhibits enhanced long-term durability due to the development of a solid, dense matrix related to traditional concrete [1].

The excessive use of the earth's resources in concrete production is the main environmental concern. Every year, the worldwide demand for aggregate, an important ingredient in concrete, exceeds 40 billion tons [10]. The marble and granite industries generate massive quantities of solid waste that are frequently disposed of in open landfills, representing a significant environmental challenge for these sectors [11]. The accumulation of this waste poses a serious threat to the environment and human health while also diminishing the available land [12]. In recent years, Waste Granite Powder (WGP) as an aggregate has been extensively utilized in various applications, including concrete bricks, clay materials, ceramic bricks and tiles, and infiltration materials [13], [14], [15], [16]. They serve as substantial substitutes for cement or natural aggregates in the manufacture of large-scale and strengthened concrete. The literature concerning the assessment of durability attributes of WGP indicates the inclusion of up to 40% granite-modified Self-Compacting Concrete (SCC) mixtures results in greater resistance to water permeability and water absorption compared to the

conventional SCC mix [17]. Incorporating dispersed granite filler diminishes overall pore volume, average pore diameter, and porosity, decreasing water absorption and penetration [18]. Thus, WGP offers the advantage of reducing water requirements and enhancing stability. This is a noteworthy benefit, as reduced water demand not only enhances the concrete quality but also augments the durability and structural performance of substitute materials. Recent investigation [1] on the Rapid Chloride Permeability Test (RCPT) indicates that concrete with a 30% WGP substitute displays lower permeability values. Furthermore, SEM and XRD analyses indicate that the compaction and density of the concrete structure are well-optimized for 15 to 30% WGP blended mix, thereby enhancing their performance compared to the control concrete [1], [19], [20]. The microstructure observed through FTIR spectra analysis of blended mortar incorporating 30% and 40% granite powder indicated enhanced hydration, leading to mechanical characteristics improvement [19]. Consequently, the durability of concrete is enhanced when WGP is used as an alternative for fine aggregate.

The past literature demonstrates the positive impacts of incorporating WGP into Self-Compacting Concrete (SCC) mixtures, such as enhanced durability, reduced water absorption, and improved mechanical properties. However, comprehensive studies on the long-term performance, application in various concrete types, and environmental and real-time applications of WGP blended concrete are lacking. This research addresses these gaps by exploring the sustainable integration of WGP in concrete production as a fine aggregate alternative, evaluating long-term performance, and establishing standardized practices for its use.

2. Research Significance

The significance of this research lies in its contribution to addressing the environmental challenges through the efficient utilization of waste materials in construction. This study evaluates the potential of using WGP as a substitute for fine aggregate in concrete. The research aims to achieve two key goals: responsible waste management within the granite industry and developing a more sustainable and long-lasting concrete by analyzing its impact on durability and microscopic structure. This would contribute significantly to both environmental conservation and the acceptance of sustainable construction techniques. The significance of this research lies in the following:

- Investigate how incorporating Waste Granite Powder (WGP) affects the durability characteristics of concrete.
- Perform a thorough microstructural examination of WGP blended concrete.
- Furthermore, analyzes correlations between durability testing results.
- To identify the optimal substitution for conventional fine aggregates by varying the percentage of WGP in a concrete mix up to 50%.
- To identify specific applications of WGP blended concrete based on the durability and microstructure properties.

3. Materials

This current research partially replaces fine aggregate with varying amounts of WGP. The section provides details on the raw materials employed in blended concrete and outlines the specimen preparation process.

3.1. Raw Materials

In this research, Ordinary Portland Cement (OPC) grade 53 is used as the binding agent, sourced from a reliable supplier. Waste Granite Powder (WGP) is obtained from a local disposal site procured in wet condition from the Mangalam granite industry located at IDA Bollaram, Hyderabad. The powder is exposed to sunlight until it is dried. The study utilizes coarse aggregate from crushed stones graded at 20 mm and 10 mm, and sand with 4.75 mm maximum grain size is sourced from a nearby vendor. The physical properties of OPC, WGP, and aggregates are assessed according to standards [21], [22] and [23] and detailed in Table 1. To enhance workability, a superplasticizer based on Sulphonated Naphthalene Formaldehyde (SNF) is employed in the concrete mixes. Additionally, potable water is utilized for both mix design and curing processes.

Figure 1 illustrates the distribution of fine aggregate and WGP grain sizes, using a mechanical sieve shaker. To assess the elemental and oxide composition in the OPC, WGP, and fine aggregate, X-ray fluorescence (XRF) tests are conducted using the Thermo Nicolet Nexus 670 dedicated instruments. The XRF determines the elemental and oxide compositions for OPC, WGP, and fine aggregate, and the oxide composition obtained is presented in Table 2.

3.2. Mix Proportions

The present research investigates the inclusion of waste granite powder (WGP) in M25-grade concrete by BIS 10262-2019 [24]. All six concrete mixtures sustain a consistent water-cement proportion of 0.5. Nevertheless, the percentage of WGP replacing fine aggregate varies from 0% to 50% by weight. Specific mix designs for each combination are detailed in Table 3.

3.3. Preparation and Curing of Specimens

Each batch of concrete is prepared in a 60kg drum mixer with precise weight measurements. First, oven-dried coarse aggregate, sand, and WGP are added. Water is introduced to moisten the mix, followed by cement after 30 seconds of blending. After 4-5 minutes of cement mixing, superplasticizer and remaining water are stirred in. The concrete rests for 1 minute while its slump is measured. Within 20 minutes, samples are molded. And after 24 hours, the cured specimens are ready for testing.

Table 1. Physical characteristics of cement, WGP, and aggregates

Experiments		Test Results	Specification as per IS 12269:2013	
Cement 53 G				
Standard Consistency (%)		29	-	
Initial Setting Time (min)		134	30 Min	
Final Setting Time (min)		178	600 Max	
Soundness (mm)		1.02	10 Max.	
Specific Gravity		3.15	-	
Fineness Modulus (m^2/kg)		309	370 Max.	
Colour		Grey	-	
Waste Granite Powder (WGP)				
Specific Gravity		2.65	IS: 4031(Part-11)	
Fineness Modulus Passing 45 µm sieve		27.5	IS: 1727	
Density (kg/m^3)		1158	-	
Colour		Light Grey	-	
Aggregates		Fine	Coarse	
		IS 4.75 mm sieve retained	20mm	10mm
Specific Gravity		2.538	2.658	2.634
Free Moisture Content (%)		5.93	Nil	Nil
Water Absorption (%)		0.903	0.235	0.294
Bulk Density (kg/m^3)	Loose	1422	1469	1427
	Compact	1585	1549	1508
Fineness Modulus		3.04	-	-

Table 2. Chemical composition of cement, WGP, and fine aggregate

S.No.	Oxides	Cement	WGP	Fine Aggregate
1	CaO	72.488 %	5.248 %	4.406 %
2	SiO_2	14.291 %	67.543 %	75.999 %
3	Fe_2O_3	6.148 %	6.778 %	2.039 %
4	SO_3	2.547 %	0.541 %	0.209 %
5	Al_2O_3	2.450 %	12.263 %	10.145 %
6	BaO	0.811 %	-	0.117 %
7	TiO_2	0.639 %	1.043 %	0.339 %
8	K_2O	0.418 %	6.181 %	6.591 %
9	MnO	0.106 %	0.120 %	0.034 %
10	SrO	0.073 %	0.060 %	0.031 %
11	ZrO_2	0.016 %	0.073 %	0.029 %
12	CuO	0.013 %	0.033 %	0.012 %
13	P_2O_5	-	-	-
14	ZnO	-	0.017 %	-
15	V_2O_5	-	0.066 %	-
16	Rb_2O	-	0.024 %	0.037%
17	Br	-	-	-
18	ThO_2	-	-	0.010 %
19	Y_2O_3	-	0.009 %	0.002 %

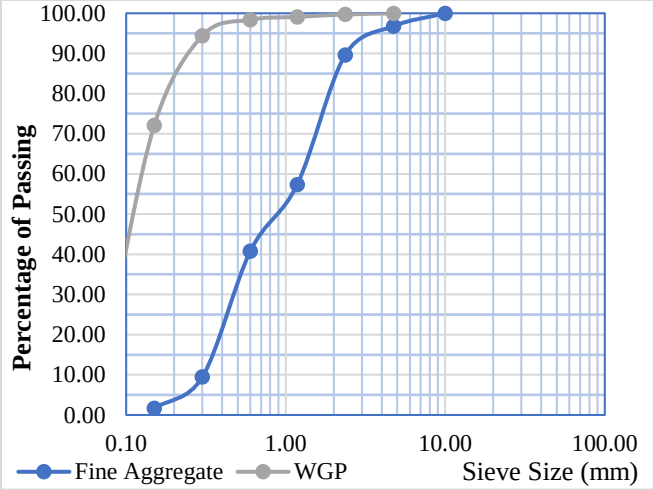

Fig. 1 Grain size distribution of fine aggregate and WGP

4. Testing Methods

In order to determine the potential of WGP as a substitute for fine aggregate, this study conducted a range of experimental tests to examine the microstructural characteristics and durability of concrete. Subsequently, the results are examined and contrasted with those of the control concrete specimens.

4.1. Fresh Properties

4.1.1. Workability

The study employs the Slump test procedure outlined in the reference [25] to measure how well the concrete mixes flowed and held together during mixing and pouring. This test measures the slump value by comparing the height of the concrete to the height of the mold after the mold is removed. The test is conducted for all concrete mixtures with different proportions of WGP using a slump cone. Measurements are taken immediately after mixing and then again at thirty and sixty minutes. The results are recorded as the average of three readings.

4.1.2. Density of Concrete

According to the specifications in [25], the weight of each mix is divided by the volume of the specimens after curing for specific durations: 7 days, 28 days, 56 days, and 90 days, to evaluate the hardened density of the concrete. The average density, recorded in kg/m³, is calculated from three specimen readings.

4.2. Durability

4.2.1. Water Absorption Test

Water absorption is measured for cube samples with dimensions of 150 mm x 150 mm x 150 mm. They undergo water curing for 28, 56, and 90 days, followed by evaluation according to the standards outlined in [26]. Following the completion of the water curing phase, the samples are carefully extracted from the curing tank and then placed on a dry cloth, away from direct sunlight exposure, until they achieve surface dryness. Subsequently, the sample's weight is recorded as W1. The water-cured samples are transferred to an oven and subjected to a 24-hour drying period at temperatures ranging from 100 to 110°C. Following this drying phase, the samples are allowed to cool to room temperature and weighed again, denoted as W2.

4.2.2. Water Penetration Test

The water penetration test is carried out on cube specimens measuring 150x150x150 mm, conforming to the standards outlined in [27]. The specimens, water-cured for 28, 56, and 90 days, are precisely positioned in a sample-holding assembly. Subsequently, they are subjected to 500 ± 50 kPa of water pressure for a period of 72 ± 2 hours. After 72-hour duration, the samples are removed from the assembly and cleaned to eliminate any excess water. Without delay, the specimen is split along the plane perpendicular to the face upon which the pressure is exerted, and the impression of water is noted. The ultimate penetration depth of water into the cubes of concrete is determined by averaging the results obtained from three separate measurements.

4.2.3. Rapid Chloride Permeability Test (RCPT)

The most crucial test for assessing the durability of concrete is RCPT. According to [28], specimens measuring a diameter of 100 mm and thickness of 50 mm are extracted from the center of cylindrical concrete samples from various mixes, all of which have been cured for 28, 56, and 90 days. Six specimens are concurrently subjected to testing, involving the insertion of discs measuring 100 mm diameter and 50 mm thickness into both a positive and a negative test cell. A 3.0% sodium chloride (NaCl) solution is added to the negative half-cell, while sodium hydroxide (NaOH) at a concentration of 0.3 normal (N) solution is added to the positive half-cell. A voltage charge of 60 ± 0.1 V is applied, and observations are recorded over 6 hours at regular intervals of 30 minutes. The quantity of charge that passes through is determined using the following formula, and the mean of three values for each sample is recorded.

4.2.4. Half-cell Potentiometer Test

According to [29], a cylindrical specimen 150 mm in diameter and 300 mm in height is employed for assessing corrosion resistance in all mix proportions of WGP. This specimen includes a 10 mm steel bar inserted in the center, with a 40 mm cover at the bottom face. Half-cell potential measurements rely on the electrical and electrolytic continuity of the reinforcement bars within the concrete, a reference electrode positioned on the concrete surface, and a voltmeter. After a curing period of 28 days, a wire is connected from the positive pole of the voltmeter to the reinforcement, while another wire from the negative pole of the voltmeter is linked to the copper-copper sulphate standard electrode placed on the concrete uppermost layer. The resulting potential difference is recorded to assess the corrosion rate by the guidelines provided in [29].

Table 3. Mix proportion of materials

Mix ID	WGP (%)	OPC (kg)	WGP (kg)	F.A (kg)	C.A (kg)		Water (kg)	Admixtures (kg)
					20mm	10mm		
WGP0	00	330	-	780	660	450	165	3.3
WGP10	10	330	78	702	660	450	165	3.3
WGP20	20	330	156	624	660	450	165	3.3
WGP30	30	330	234	546	660	450	165	3.3
WGP40	40	330	312	468	660	450	165	3.3
WGP50	50	330	390	390	660	450	165	3.3

4.3. Microstructure Analyses

4.3.1. Scanning Electron Microscopy (SEM) and Energy-Dispersive X-Ray Spectroscopy (EDS)

The microstructure analysis of various WGP concrete samples is conducted by using the crushed compressive strength specimens. These samples are carefully collected and then passed through a 150 µm sieve. The resulting particles from the sample are then deposited onto a carbon tape and wrapped with gold for Scanning Electron Microscopy (SEM) evaluation. SEM and EDS represent advanced techniques employed to examine the morphology of concrete. SEM delivers high-resolution images of the concrete's microstructure, while EDS enables the identification and quantification of the elements within the concrete. These analyses are carried out on all the concrete mixes using a HITACHI S – 3700N instrument. The SEM analysis employs a scale range of 10 µm, with a magnification resolution of x 1000 and 400 µm, with an x 500 magnification rate.

4.3.2. Fourier Transform Infrared (FTIR) Spectroscopy

The chemical composition of a concrete mixture is examined using Fourier Transform Infrared (FTIR) spectroscopy. In this process, concrete samples are first dried and finely powdered. The resulting sample is then subjected to analysis using a PerkinElmer Spectrum Two FTIR spectrometer, and the infrared spectra are obtained across the spectral range from 400 to 4000 cm^{-1}.

The FTIR spectrum is accurately examined to identify the different chemicals present in the concrete. The functional groups present in the concrete are identified and quantified based on spectral peaks.

5. Results and Discussions

5.1 Fresh Properties

5.1.1. Workability

Figure 2 illustrates the workability of freshly mixed concrete for various mixtures at different time intervals: immediately after mixing, 30 minutes, and 60 minutes. Across all mixtures, a notable decrease in slump is observed over time, with this trend being more pronounced at higher WGP substitution rates. The control mix (WGP0) exhibits the highest workability, while the WGP50 blend is the least workable. The slump loss for the control mix is 130 mm, compared to 110 mm, 75 mm, 35 mm, and 20 mm for WGP10, WGP20, WGP30, and WGP40 mixes, respectively. As the WGP proportion rises, the viscosity and flow resistance of the mix increase, resulting in a lower slump value. The main cause of this decline is an increase in water demand, which is impacted due to aggregates' size, texture, specific surface area, and shape [30]. The concrete's workability significantly reduces as more water is absorbed, while the cement content remains constant [31].

5.1.2. Density of Concrete

Figure 3 shows the density of concrete containing WGP, which increases significantly with the age of curing at 7, 28, 56, and 90 days for the mixtures (WGP10 to WGP40) as the substitution rate rises, compared to the control mix (WGP0). The reason for this increase is that WGP has a smaller particle size distribution than sand, resulting in more densely packed concrete with reduced mortar porosity.

However, a decrease in density is observed in the WGP50 mix. This reduction is due to the rough, coarse, and angular properties of WGP, which introduce air content and voids, thereby lowering the initial density of the concrete. Additionally, WGP has a lower specific gravity than fine aggregate [32], contributing to the lower density observed in the WGP50 mix, as shown in Table 4.

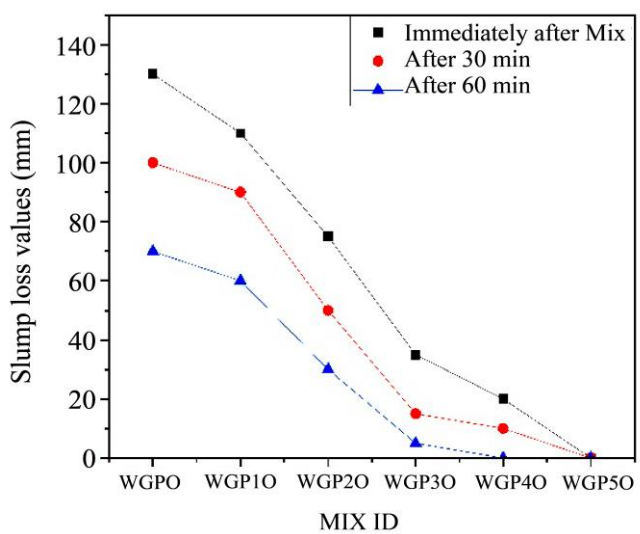

Fig. 2 Slump loss value of WGP blended concrete

5.2. Durability Property

5.2.1. Water Absorption Test

In contrast to the control mix (WGP0), the water absorption initially exhibits a notable reduction for WGP blended mixes (WGP10 to WGP40). Subsequently, the water absorption increases as the substitution level increases for the mix WGP50 at 28, 56, and 90 days of aging, as depicted in Figure 4. The reduction in water absorption for WGP10 to WGP40 is 12.97%, 15.56%, 19.88%, and 24.78% when contrasted to the control mix (WGP0) at 28 days, respectively. Identical trends continue beyond 56 and 90 days of curing. The decline in absorption of water may be ascribed to WGP's filler effect, which promotes the development of C-S-H gel, enhances the density of concrete, and decreases porosity.

The minimal absorption of water observed in the mix with 40% replacement can be attributed to the interconnectivity of interpores, which restricts water permeability [33]. The rise in water absorption beyond 40% WGP substitution as fine aggregate is linked to the formation of numerous voids within the blended concrete. This phenomenon creates an inadequacy of cement paste, contributing to the development of an unfavorable microstructure with voids in the blended concrete mix (WGP50), ultimately resulting in increased water absorption [17].

5.2.2. Water Penetration Test

The water penetration performance of both the control mix (WGP0) and WGP blended concrete mix (WGP10 to WGP50) is illustrated in Figure 5 for a curing period of 28, 56, and 90 days. Upon completion of the 28-day curing phase, the water penetration depths are as follows: 23.5 mm for the control mix, and 19.5 mm, 18 mm, 17 mm, 16.5 mm, and 18.5 mm for WGP10, WGP20, WGP30, WGP40, and WGP50, respectively. In contrast to the conventional mix (WGP0), the percentage reduction is 17.02%, 23.40%, 29.66%, 29.79%, and 21.28% of the blended mix (WGP10 to WGP50), respectively.

Upon 56 and 90 days of ageing, similar trends are observed. The filler effect of WGP particles, which occupy voids and restrict water penetration [34], can be linked to the decrease in water penetration depth. However, a further increase in the substitution level of WGP in the concrete mix (WGP50) leads to greater water penetration.

This is due to the impact of a higher proportion of WGP on the water-cement percentage, leading to porosity during hydration and possibly inadequate gradation and the finer texture of the WGP, causing a reduced binding paste and leading to the formation of porous blended concrete with increased voids. [1], [34]. In conclusion, the fine particles of WGP act as fillers, significantly reducing water penetration depth and achieving a denser mixture.

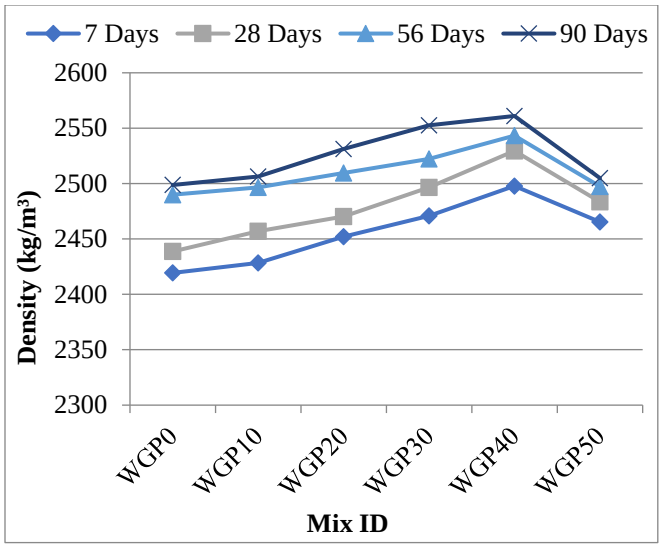

Fig. 3 Variations of density of WGP blended concrete

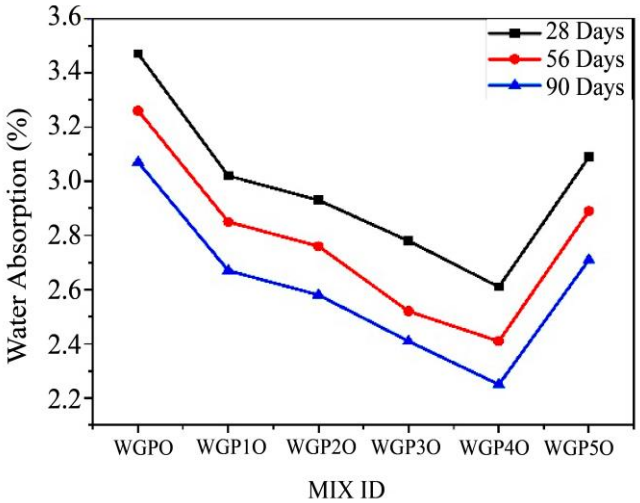

Fig. 4 Water absorption after curing interval of 28, 56, and 90 days

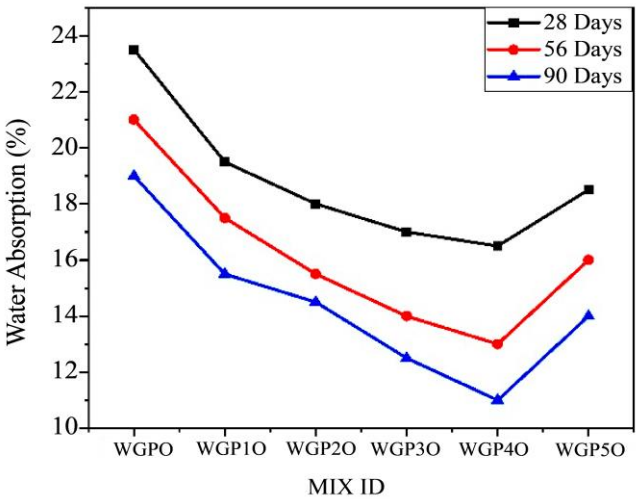

Fig. 5 Water Penetration at curing ages 28, 56, and 90 days

5.2.3. Rapid Chloride Permeability Test (RCPT)

The outcomes from the RCPT conducted on WGP blended concrete specimens, as illustrated in Figure 6, demonstrated significantly improved resistance compared to control specimens at 28, 56, and 90 days. After the curing period of 28 days, there is a substantial decrease in the total charge passed, with percentages of WGP blended mix (WGP10 to WGP50) 9.50%, 10.43%, 15.72%, 17.60%, and 16.67% less in response to the control mix (WGP0). The test results indicated an inverse relationship between the chloride ion permeability of the mixture and the WGP replacement level; as the WGP replacement level increases, the permeability to chloride ions decreases. However, the WGP40 blended mix exhibited the highest reduction of chloride ion permeability in comparison to the conventional mix (WGP0). The substantial reduction in charge passed is due to the micro filler particles of WGP, which contribute to the formation of a compact microstructure that hinders the movement of charges. With a further rise in the WGP substitution level beyond 40%, the permeability of chloride ions also increases. This can be attributed to insufficient densification, which results in a highly porous microstructure and a fragmented pore arrangement, thereby enhancing permeability to chloride ions. According to the guidelines [28], concrete containing WGP is characterized as 'very low' chloride ion penetrable concrete based on the charge passed in coulombs.

5.2.4. Half-Cell Potentiometer Test (HCP)

The findings from the HCP test at 28 days, comparing the control mix (WGP0) with WGP blended mixes, are depicted in Figure 7. Results indicate that WGP blends (WGP10, WGP20, and WGP30) demonstrate reduced corrosion potential by 13.61%, 3.85%, and 0.78%, respectively, compared to the control mix (WGP0). This decline in corrosion potential is attributed to effective gradation, void-filling by WGP microparticles, and the existence of a high SiO_2 percentage, which aids in generating extra calcium silicate hydrate (C-S-H) throughout the cement hardening phase. Consequently, a denser and more compact cement matrix forms, acting as a protective barrier around reinforced steel bars. This densification and reduced permeability help restrict water ingress toward the steel reinforcement, thereby aiding in steel bar passivation and improving corrosion resistance. However, with an increase in the WGP substitution rate, corrosion potential tends to rise. This escalation may be attributed to the introduction of highly reactive elements like feldspar and mica present in WGP, which could potentially diminish steel passivation effectiveness, leading to a higher corrosion potential.

5.3. Microstructural Analysis

5.3.1. SEM – EDS

SEM-EDS analysis is conducted on all mixtures utilized in this study, as depicted in Figure 9. SEM images in Figure 8, at a resolution of 20 microns, depict the presence of a calcium-silicate-hydrate gel (C-S-H), calcium hydroxide (C-H), and voids in the samples after 28 days. Particularly, specimens WGP30 and WGP40 display a continuous fibrous network of calcium silicate hydrate (C-S-H). Aluminium appears in every sample, indicating the presence of ettringite. Moreover, white particles are observed, indicating either non-hydrated cement or a brighter C-S-H gel surrounding the aggregates.

Table 4. Variation in Density (kg/m^3) of blended concrete at different curing ages

MIX ID	7 Days	28 Days	56 Days	90 Days
WGP0	2419.358	2438.66667	2489.988	2498.724
WGP10	2428.258	2456.87654	2496.593	2506.444
WGP20	2452.144	2470.24691	2509.679	2531.247
WGP30	2470.847	2496.44444	2522.279	2552.457
WGP40	2497.819	2529.50617	2543.284	2561.049
WGP50	2465.423	2483.45679	2497.358	2504.877

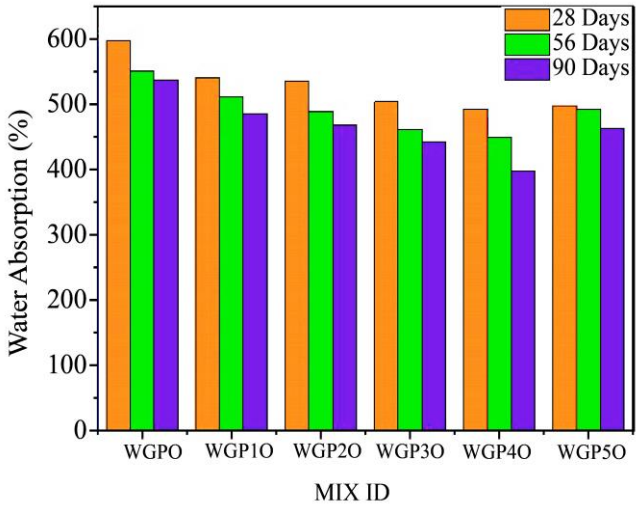

Fig. 6 RCPT of Concrete at Various Curing Ages

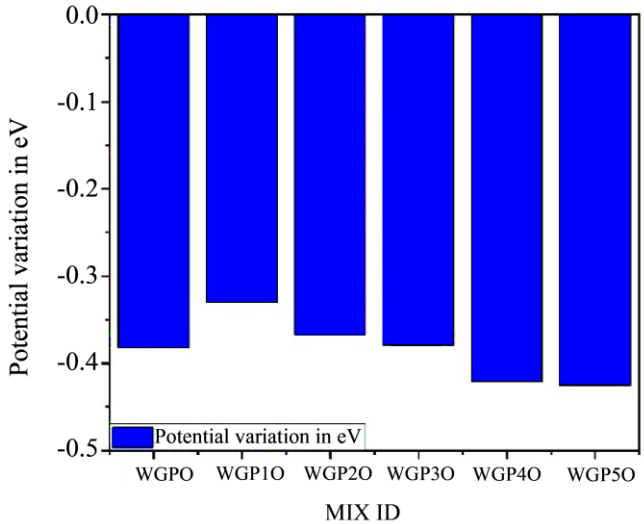

Fig. 7 Half-Cell Potentiometer test at 28 days of curing

EDS test results, extracted from various spots within the SEM images, measured the elemental composition of the different concrete mixes. Table 5 illustrates the predominant element present across all concrete mixes. From the EDS analysis, the Si/Al ratio is determined based on the atomic weight percentages for all mixes and is shown in Table 5. The Si/Al ratio, calculated from the atomic weight percentages, is 5.86, 3.86, 4.78, 5.88, 6.91, and 3.88 across all the mixes (from WGP0 to WGP50). Among all the blends, WGP30 and WGP40 exhibited the highest Si/Al ratio, primarily due to the fine particle size of WGP, which, in turn, encourages better geopolymerization and network connectivity [35]. In the SEM images, hexagonal-shaped plates indicated the presence of C-H, predominantly stacked on top of each other and are distinctly visible only in WGP40 at 28 days. WGP30 exhibited a network of calcium silicate hydrate and minor calcium hydroxide phases, along with some noticeable pores. Conversely, WGP0, WGP10, WGP20, and WGP50 showed reduced C-S-H generation and a minor change in pore structure.

5.3.2. Fourier Transform Infrared (FTIR) Spectroscopy

The results of the Fourier-transform infrared spectroscopy (FTIR) analysis for six distinct samples after the 28-day curing period are shown in Figure 10, with an absorbance band ranging from 4000 to 450 cm^{-1}. The peaks occurring at 3400 cm^{-1} correspond to the O-H vibration of calcium hydroxide (CH), and 1600-1650 cm^{-1} align with the asymmetric vibration peak (v2) of H-O-H bending associated with water molecules, respectively [36]. The strong bands around 1400-1420 cm^{-1} and 872 cm^{-1} are allied with carbonates arising due to the carbonation of portlandite [37]. The dip around 453-725 cm^{-1} is assigned as Si-O bending vibrations due to quartz from sand. Notably, the band at 1000 cm^{-1}, observed when utilizing granite powder instead of sand, indicates a dominance of Si-O-Si bonding over Si-O-Al bonding. As a result, it can be deduced from these results that the introduction of WGP modifies the hydration reaction, thereby enhancing the strength of the blended concrete.

The peak classifications are displayed in Table 6. The peaks shift to a higher wavenumber range of 1000 - 1033 cm^{-1} for the blended mix WGP20, WGP30, and WGP40, respectively. This shift signifies the initiation of geopolymerization within the material, indicating that the structural modification has transformed the crystalline forms of alumino-silicates ($SiO_2.Al_2O_3$) into amorphous tetrahedra of SiO_4 and AlO_4 [35]. Since the changes in peak positions indicate the reorganization of silicates into geopolymeric structures.The appearance of new bands in the 1000 to 1200 cm-1 range indicates the development of Si-O-Al linkages characteristic of geopolymers. They reorganize and form new chemical bonds, creating a complex lattice of interconnected Si-O-Al-O linkages., known as the geopolymeric gel.

This geopolymeric gel acts as a binding phase that solidifies and contributes to the material's structure. It replaces the original crystalline silicate structure with an amorphous or semi-crystalline geopolymeric matrix. The most pronounced band shift is observed in WGP30 and WGP40 mixes, indicating maximum geopolymerization and enhanced network connectivity in these compositions of materials. A maximum degree of geopolymerization typically denotes a more thorough transformation of the raw materials into the geopolymer phase, resulting in enhanced microstructure, strength, and durability of the material.

The study has effectively shown that substituting WGP for a portion of the fine aggregate in concrete production not only meets but also surpasses durability requirements set by conventional and state-of-the-art techniques. The combination of an optimized mix design, advanced characterization methods, and comprehensive durability testing with thorough correlation analysis has enabled us to achieve superior results. Additionally, the microstructure analysis and environmental and real-time application of blended concrete further reinforce the viability of using WGP in concrete production, providing a sustainable and durable solution for the construction industry.

Table 5. Si/Al atomic ratio from EDS analysis

Elements	WGP0	WGP10	WGP20	WGP30	WGP40	WGP50
Si	41.63	29.02	63.40	43.01	65.86	37.80
Ca	42.930	55.43	11.95	43.02	16.34	41.68
Al	7.100	7.52	13.26	7.31	9.53	9.73
K	1.860	2.42	6.65	2.25	6.01	3.23
Si/Al	5.86	3.86	4.78	5.88	6.91	3.88

Table 6. FTIR peak classifications

S.No.	Wave numbers (cm^{-1})	Possible assignment
1	3400-3650	O-H stretching of calcium hydroxide (CH)
2	1600-1650	v2 bending of H2O
3	1000-1200	Si-O-T stretching vibrations of alumino-silicate
4	1400-1420	v3 stretching vibration peak of C-O
5	871-872	v2 stretching of carbonate
6	453-725	Si-O bending vibrations due to quartz

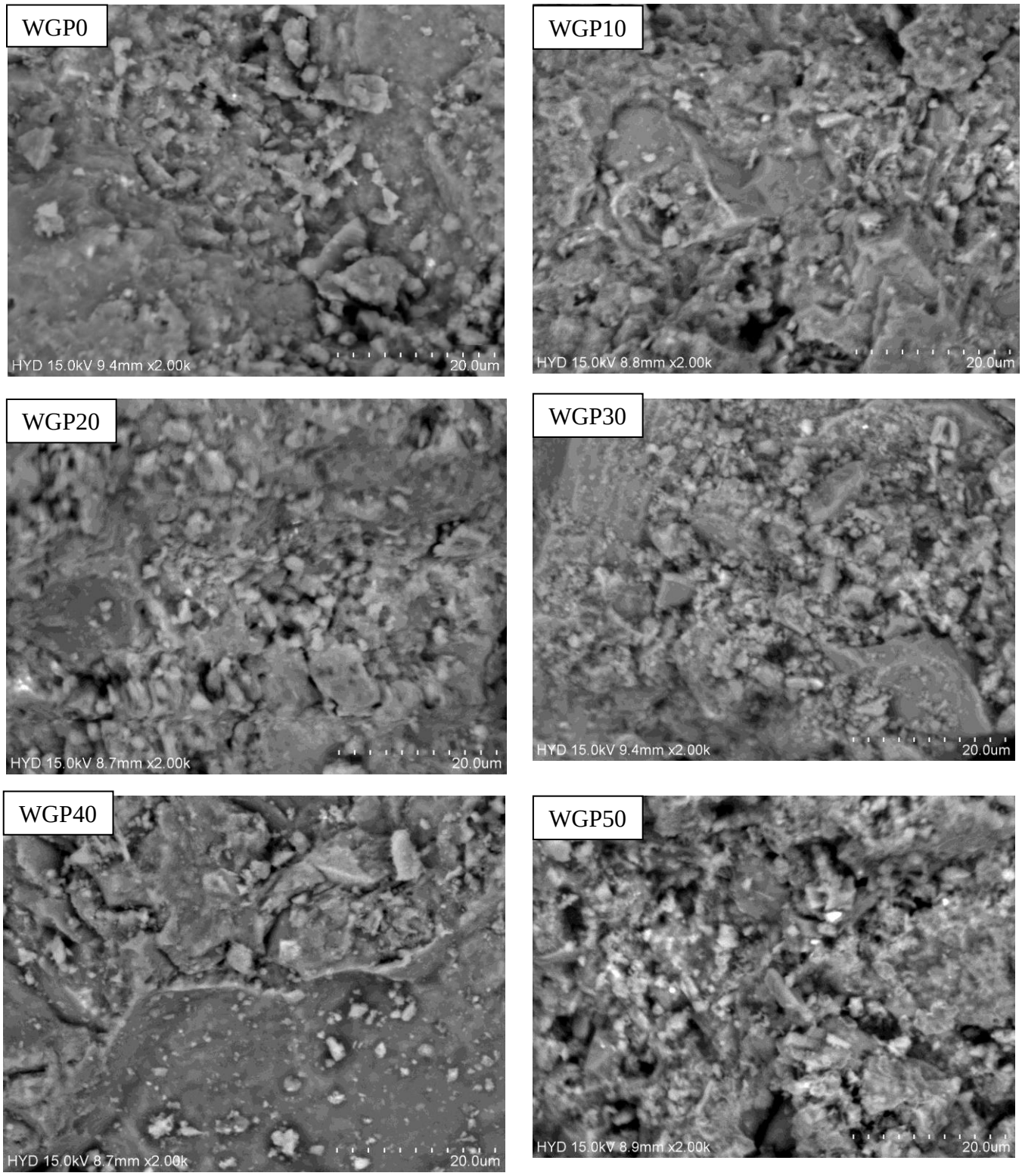

Fig. 8 SEM micrographs at 28 days

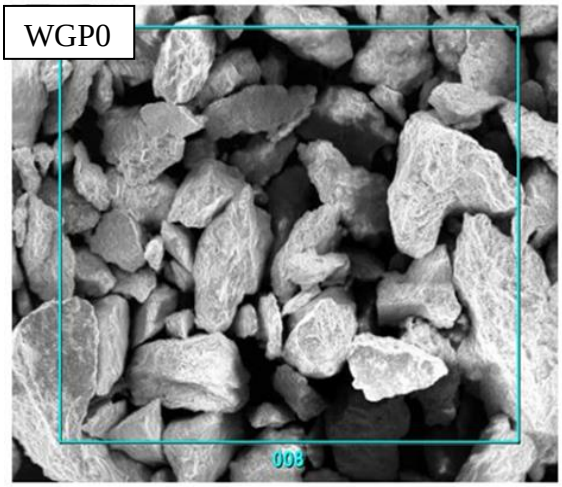
WGP0
008

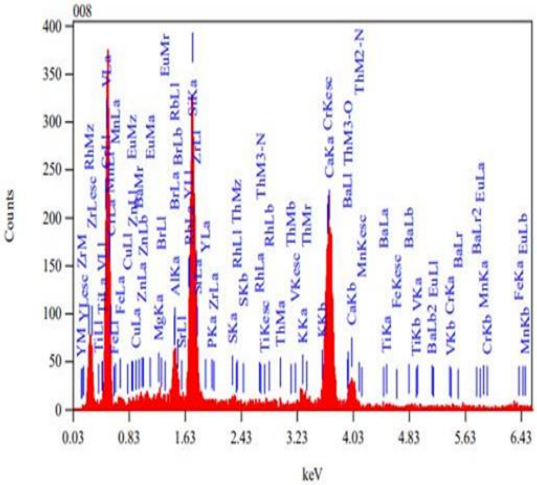
008
Counts
keV

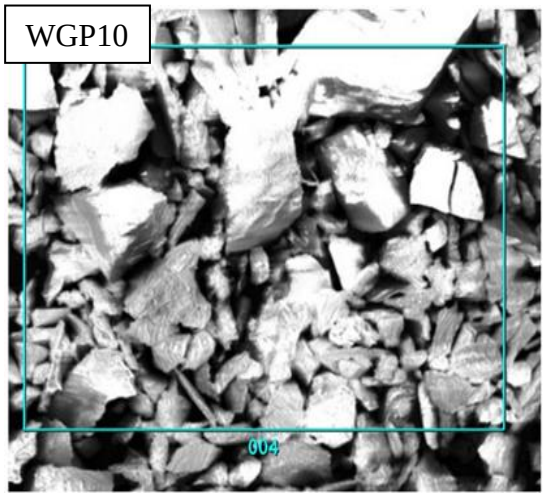
WGP10
004

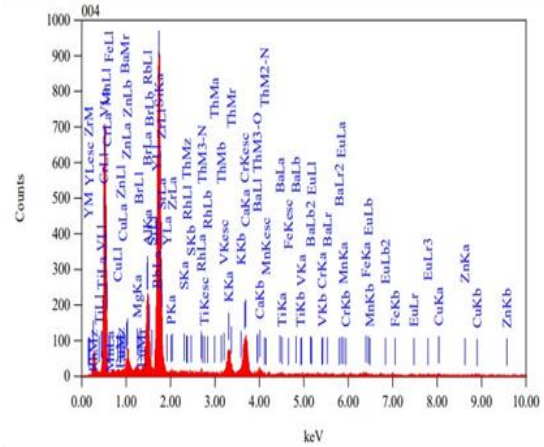
004
Counts
keV

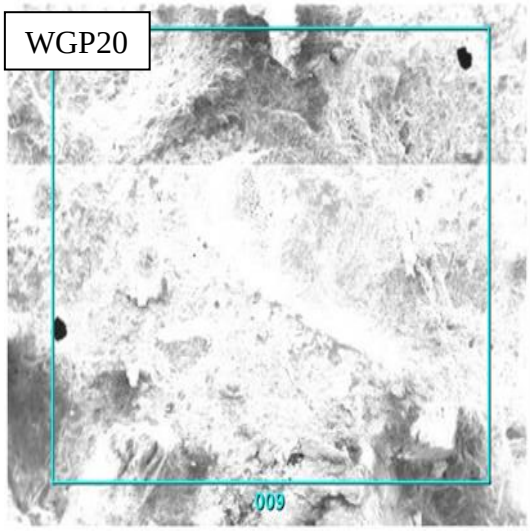
WGP20
009

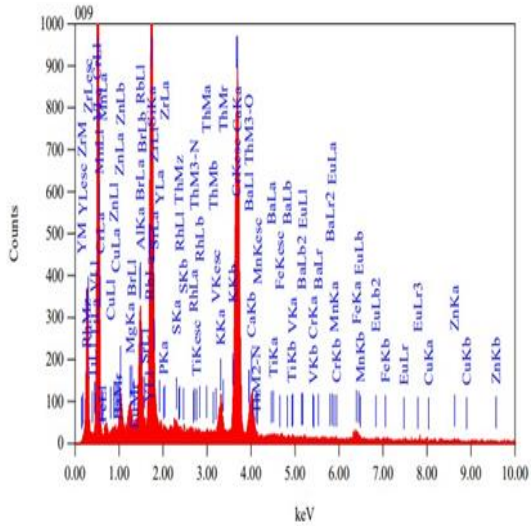
009
Counts
keV

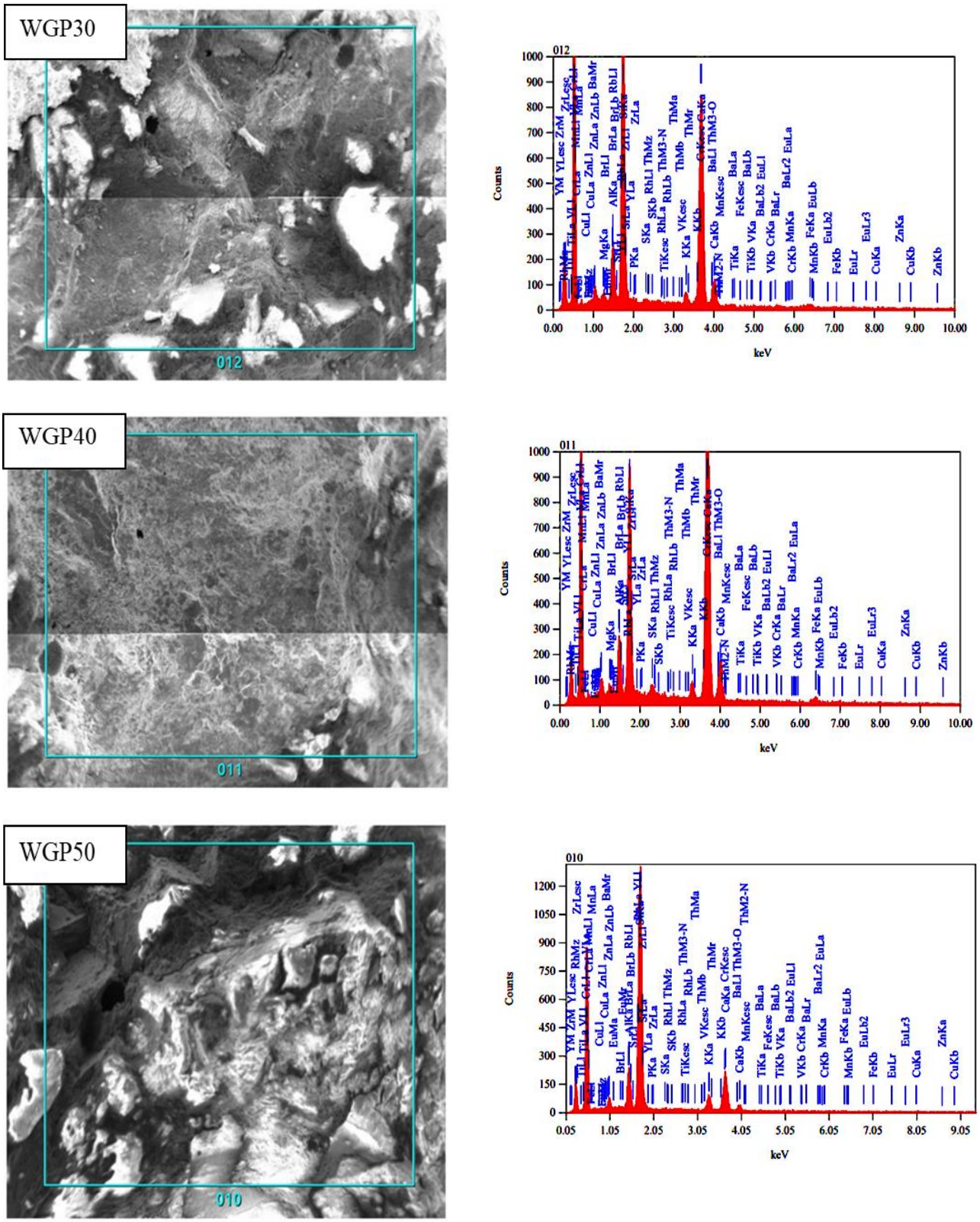

Fig. 9 SEM-EDS micrographs at 28 days

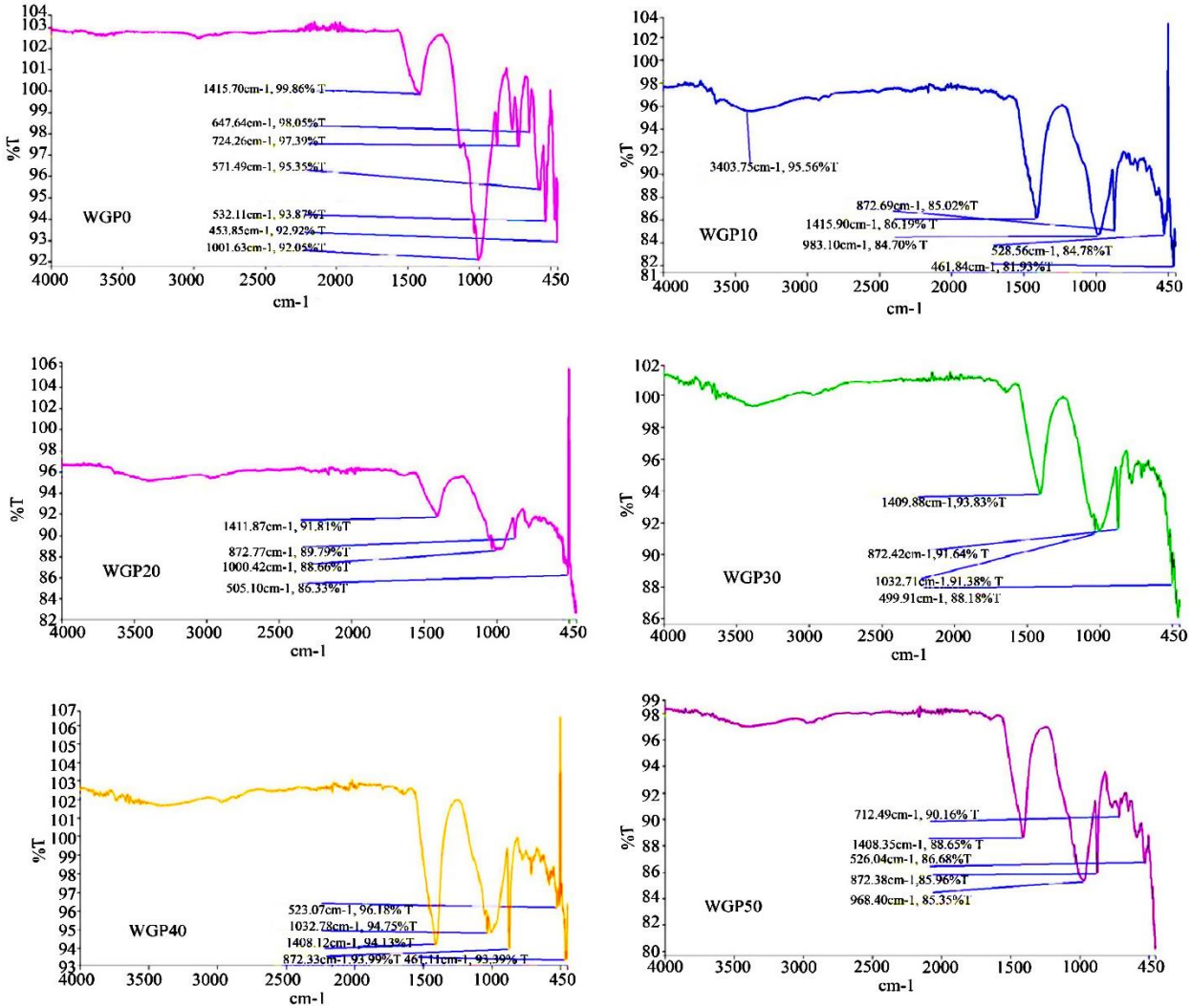

Fig. 10 FTIR analysis at 28 days

5.3. Correlations

This section comprehensively explores the relationships among durability properties. The analysis systematically outlines these relationships: destructive vs destructive tests (WA vs WP, WA vs RCPT, WP vs RCPT). Figures 11 to 13 summarize these correlations.

5.3.1. Correlation between WP and WA

In Figure 11, a strong regression coefficient (R) of 0.93 is observed for the correlation between WP and WA in WGP10 to WGP50 blended concrete, contrasting with the control mix (WGP0). Initially, WP and WA values decrease with increasing WGP content, stabilizing or slightly increasing at higher replacement levels. This trend could be attributed to finer WGP particles enabling denser packing, limiting interconnected voids, and reducing overall porosity, thereby minimizing water ingress. Additionally, the rougher surface characteristics of waste granite particles enhance bonding with cement paste, further reducing the pore network.

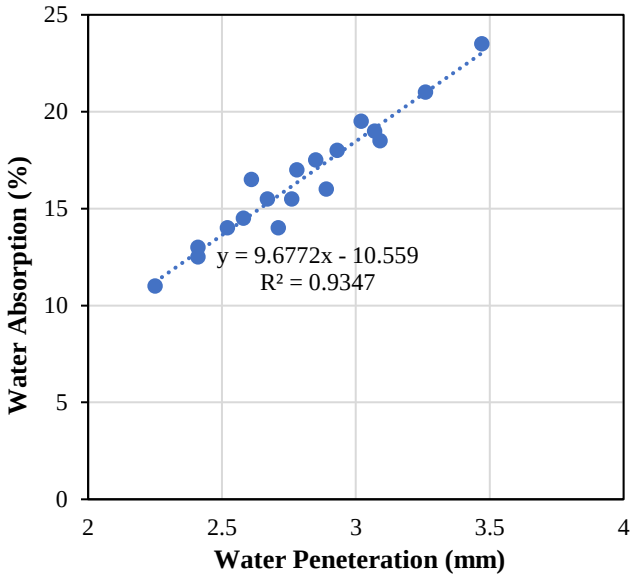

Fig. 11 Correlation between WA and WP

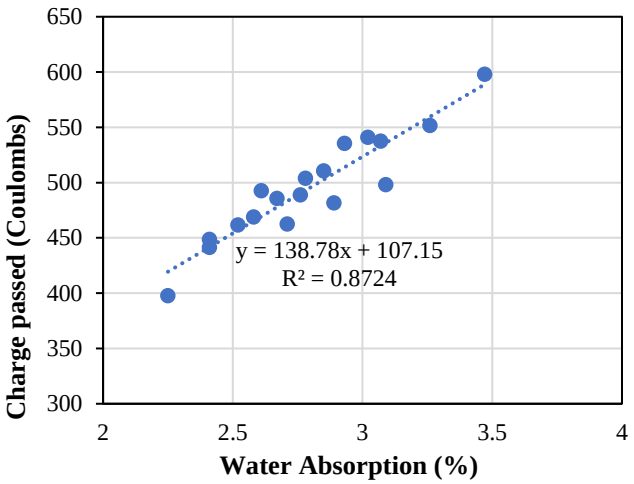

Fig. 12 Correlation between WA and RCPT

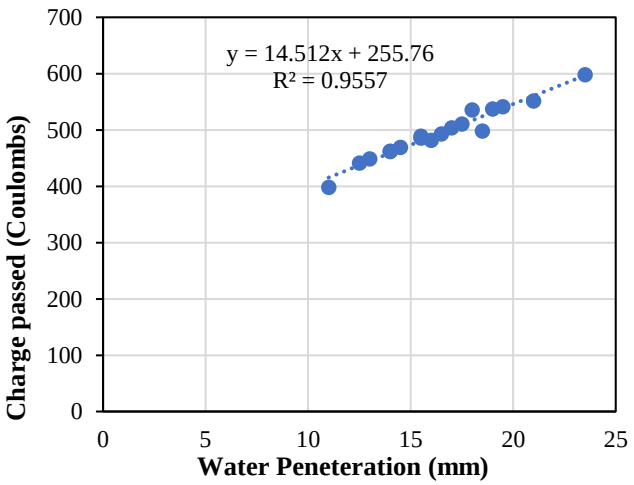

Fig. 13 Correlation between WP and RCPT

5.3.2. Correlation between WA and RCPT

Figure 12 illustrates the relationship between WA and RCPT, where all pooled data are collectively plotted. An observed strong regression coefficient (R) of 0.87 between WA and RCPT in WGP0 to WGP50. The incorporation of waste granite particles in concrete offers significant advantages in terms of reduced porosity and improved durability in WGP blended concrete (WGP10 to WGP50). The hydration process of cement may also be influenced by waste granite powder, leading to a denser and more complete hydration reaction, further reducing water absorption.

5.3.3. Correlation between WP and RCPT

In Figure 13, a strong correlation is observed with a regression coefficient (R) of 0.95 between WP and RCPT in concrete mixtures ranging from WGP0 to WGP50. The lower RCPT values observed in WGP blended concrete (WGP10 to WGP50) are attributed to the fine particles of waste granite powder serving as fillers. This enhancement of the pore structure creates a denser, less permeable concrete matrix that effectively prevents chloride ion penetration.

5.4. Specific Application based on Various Parameters

This section examines the potential utilization of WGP blended concrete based on a detailed assessment of its durability properties and microstructural characteristics. The comprehensive evaluation exhibits valuable insights into the material's suitability for several construction situations, its long-term performance, and its environmental benefits.

- Durability properties demonstrate that WGP blended concrete provides improved resistance to water absorption and penetration. This makes it especially well-suited for precast elements exposed to various weather conditions. For instance, using WGP concrete blocks on exterior walls of buildings exposed to rain or moisture can effectively prevent water seepage and extend the longevity of the structure. Furthermore, the outcomes of the RCPT and HCP tests show that WGP blended concrete is appropriate for use in marine surroundings or situations in which de-icing salts are utilized. This highlights its ability to resist corrosion caused by chloride ion penetration.
- SEM-EDS and FTIR microstructural analysis demonstrate that WGP improves the concrete's microstructure, leading to better density and exceptional resistance to chemical attack. This interprets outstanding long-term durability in adverse environments, making it the excellent choice for essential load-bearing elements like parking tiles, exterior walls, and cost-effective flooring applications. WGP's adaptability extends to sidewalks, pavements, and similar applications, demanding both resilience and strength.

6. Conclusion

The present research examines the viability of utilizing Waste Granite Powder (WGP) as a partial replacement for fine aggregate in concrete, focusing specifically on replacement levels ranging from 10% to 50%. The study determines whether WGP is a feasible substitute material for concrete by analyzing its effects on the material's microstructural features and durability. Therefore, from the experimental outcomes, the study concludes the following:

- The durability of WGP blend concrete proves beneficial in enhancing water absorption and penetration resistance up to 40% replacement in concrete. This improvement is attributed to WGP's filler effect, leading to a denser microstructure and effective binding, reducing porosity. However, exceeding the 40% replacement results in compromised microstructure, leading to increased water absorption and penetration.
- WGP significantly enhances concrete's chloride ion resistance up to 40% replacement, with WGP40 exhibiting the optimal performance. Beyond 40%, porosity and fragmented pores increase permeability. This highlights WGP40 as ideal for maximizing chloride resistance while meeting ‘very low chloride ion penetrability’ as per ASTM C1202-12.

- When associated with the conventional mix, the HCP test results of up to 30% replacement enhance steel corrosion resistance due to denser microstructure, void filling, and SiO_2-driven C-S-H formation. Beyond 30%, highly reactive elements in WGP compromise passivation and increase corrosion. This highlights 30% as the optimal WGP level for maximizing steel protection.
- Microstructure analysis (SEM-EDS) reveals optimal geopolymerization at 40% WGP replacement (WGP40), evidenced by a continuous C-S-H gel network, high Si/Al ratio, and prominent 1000 cm^{-1} band in FTIR. This indicates stronger binding, denser microstructure, and potentially enhanced material properties like strength and durability.
- Concrete incorporating WGP demonstrates significant correlations in its durability properties. This strong relationship is attributed to finer WGP particles facilitating denser packing, improved bonding with cement paste, and a refined pore structure.
- With its enhanced properties, WGP blended concrete proves advantageous for low-rise structures, road pavements, footbridges, and precast elements in recreational areas, offering a balance of strength and durability. Its application not only improves construction performance but also aligns with eco-conscious building practices, promoting sustainability.

Based on extensive studies on concrete durability and microstructure, replacing a portion of the fine aggregates with WGP suggests that substituting up to 40% can yield beneficial results. However, real-world application through field trials is essential to definitively confirm the adequacy of this approach for sustainable construction.

Acknowledgement

The authors extend their sincere gratitude to Mangalam Granite Industry Limited, located at IDA Bollaram, Hyderabad, India, for generously providing Waste Granite Powder (Slurry) and to UltraTech Cement for supplying cement (OPC 53 grade) essential for this study.

References

[1] Kishan Lal Jain, Gaurav Sancheti, and Lalit Kumar Gupta, "Durability Performance of Waste Granite and Glass Powder Added to Concrete," *Construction and Building Materials*, vol. 252, 2020. [CrossRef] [Google Scholar] [Publisher Link]

[2] L.G. Li et al., "Adding Granite Dust as Paste Replacement to Improve Durability and Dimensional Stability of Mortar," *Powder Technology*, vol. 333, pp. 269–276, 2018. [CrossRef] [Google Scholar] [Publisher Link]

[3] Sawekchai Tangaramvong et al., "The Influences of Granite Industry Waste on Concrete Properties with Different Strength Grades," *Case Studies in Construction Materials*, vol. 15, pp. 1-12, 2021. [CrossRef] [Google Scholar] [Publisher Link]

[4] Başak Mesci, Semra Çoruh, and Osman Nuri Ergun, "Use of Selected Industrial Waste Materials in the Concrete Mixture," *Environmental Progress & Sustainable Energy*, vol. 30, no. 3, pp. 368–376, 2011. [CrossRef] [Google Scholar] [Publisher Link]

[5] Manoj Kumar Dash, Sanjaya Kumar Patro, and Ashoke Kumar Rath, "Sustainable Use of Industrial-Waste as Partial Replacement of Fine Aggregate for Preparation of Concrete – A Review," *International Journal of Sustainable Built Environment*, vol. 5, no. 2, pp. 484–516, 2016. [CrossRef] [Google Scholar] [Publisher Link]

[6] Malek Batayneh, Iqbal Marie, and Ibrahim Asi, "Use of Selected Waste Materials in Concrete Mixes," *Waste Management*, vol. 27, no. 12, pp. 1870–1876, 2007. [CrossRef] [Google Scholar] [Publisher Link]

[7] L.G. Li et al., "Filler Technology of Adding Granite Dust to Reduce Cement Content and Increase Strength of Mortar," *Powder Technology*, vol. 342, pp. 388–396, 2019. [CrossRef] [Google Scholar] [Publisher Link]

[8] M. Nehdi, J. Duquette, and A. El Damatty, "Performance of Rice Husk Ash Produced Using a New Technology as a Mineral Admixture in Concrete," *Cement and Concrete Research*, vol. 33, no. 8, pp. 1203–1210, 2003. [CrossRef] [Google Scholar] [Publisher Link]

[9] Maria Chiara Bignozzi et al., "Sustainable Cement for Green Buildings Construction," *Procedia Engineering*, vol. 21, pp. 915–921, 2011. [CrossRef] [Google Scholar] [Publisher Link]

[10] Vivian W.Y. Tam, Mahfooz Soomro, and Ana Catarina Jorge Evangelista, "A Review of Recycled Aggregate in Concrete Applications (2000–2017)," *Construction and Building Materials*, vol. 172, pp. 272–292, 2018. [CrossRef] [Google Scholar] [Publisher Link]

[11] Iman Taji et al., "Application of Statistical Analysis to Evaluate the Corrosion Resistance of Steel Rebars Embedded in Concrete with Marble and Granite Waste Dust," *Journal of Cleaner Production*, vol. 210, pp. 837–846, 2019. [CrossRef] [Google Scholar] [Publisher Link]

[12] K. Aarthi, and K. Arunachalam, "Durability Studies on Fiber Reinforced Self-Compacting Concrete with Sustainable Wastes," *Journal of Cleaner Production*, vol. 174, pp. 247–255, 2018. [CrossRef] [Google Scholar] [Publisher Link]

[13] K. Balaji Rao, V. Bhaskar Desai, and D. Jagan Mohan, "Probabilistic Analysis of Mode II Fracture of Concrete with Crushed Granite Stone Fine Aggregate Replacing Sand," *Construction and Building Materials*, vol. 27, no. 1, pp. 319–330, 2012. [CrossRef] [Google Scholar] [Publisher Link]

[14] Hanifi Binici et al., "Durability of Concrete Made with Granite and Marble as Recycle Aggregates," *Journal of Materials Processing Technology*, vol. 208, no. 1–3, pp. 299–308, 2008. [CrossRef] [Google Scholar] [Publisher Link]

[15] Blasius Ngayakamo, Abdulhakeem Bello, and Azikiwe Peter Onwualu, "Valorization of Granite Waste Powder as a Secondary Flux Material for Sustainable Production of Ceramic Tiles," *Cleaner Materials*, vol. 4, pp. 1-8, 2022. [CrossRef] [Google Scholar] [Publisher Link]

[16] F. Saboya, G.C. Xavier, and J. Alexandre, "The Use of the Powder Marble by-Product to Enhance the Properties of Brick Ceramic," *Construction and Building Materials*, vol. 21, no. 10, pp. 1950–1960, 2007. [CrossRef] [Google Scholar] [Publisher Link]

[17] Abhishek Jain, Rajesh Gupta, and Sandeep Chaudhary, "Performance of Self-Compacting Concrete Comprising Granite Cutting Waste as Fine Aggregate," *Construction and Building Materials*, vol. 221, pp. 539–552, 2019. [CrossRef] [Google Scholar] [Publisher Link]

[18] Grzegorz Prokopski, Vitaliy Marchuk, and Andriy Huts, "The Effect of Using Granite Dust as a Component of Concrete Mixture," *Case Studies in Construction Materials*, vol. 13, pp. 1-7, 2020. [CrossRef] [Google Scholar] [Publisher Link]

[19] Lalit Kumar Gupta, and Ashok Kumar Vyas, "Impact on Mechanical Properties of Cement Sand Mortar Containing Waste Granite Powder," *Construction and Building Materials*, vol. 191, pp. 155-164, 2018. [CrossRef] [Google Scholar] [Publisher Link]

[20] M. Vijayalakshmi, A.S.S. Sekar, and G. Ganesh Prabhu, "Strength and Durability Properties of Concrete Made with Granite Industry Waste," *Construction and Building Materials*, vol. 46, pp. 1–7, 2013. [CrossRef] [Google Scholar] [Publisher Link]

[21] BIS: 12269: 2013, Indian Standard 53 Grade Ordinary Portland Cement—Specification, New Delhi: Bureau of Indian Standards, 2013. [Online]. Available: https://www.services.bis.gov.in/php/BIS_2.0/bisconnect/knowyourstandards/Indian_standards/isdetails/OTg=

[22] BIS: 4031 (Part 11), 'Methods of Physical Tests for Hydraulic Cement Part 11 Determination of Density (First Revision),' New Delhi: Bureau of Indian Standards, 1988. [Online]. Available: https://www.services.bis.gov.in/php/BIS_2.0/bisconnect/standard_review/Standard_review/Isdetails?ID=MTA2NjM%3D

[23] BIS 2386 (Part 3), Methods of test for Aggregates for Concrete, New Delhi: Bureau of Indian Standards, 1963. [Online]. Available: https://law.resource.org/pub/in/bis/S03/is.2386.1.1963.pdf

[24] BIS 10262: 2019, Concrete Mix Proportioning-Guidelines (Second Revision), Bureau of Indian Standards, New Delhi, 2019. [Online]. Available: https://archive.org/details/gov.in.is.10262.2019

[25] BIS 1199: 1959, Methods of Sampling and Analysis of Concrete, Bureau of Indian Standards, New Delhi, 2023. [Online]. Available: https://www.services.bis.gov.in/php/BIS_2.0/bisconnect/standard_review/Standard_review/Isdetails?ID=MzIxMQ%3D%3D

[26] BIS 1124: 1974, Method of Test for Determination of Water Absorption, Apparent Specific Gravity, and Porosity of Natural Building Stones, New Delhi: Bureau of Indian Standards, 1974. [Online]. Available: https://www.services.bis.gov.in/php/BIS_2.0/bisconnect/standard_review/Standard_review/Isdetails?ID=MjI5NA%3D%3D

[27] BIS: 516 (Part 2/Sec 1): 2018, Hardened Concrete — Methods of Test Part 2 Properties of Hardened Concrete other than Strength Section 1 Density of Hardened Concrete and Depth of Water Penetration Under Pressure (First Revision), New Delhi: Bureau of Indian Standards, 2018. [Online]. Available: https://www.services.bis.gov.in/php/BIS_2.0/bisconnect/standard_review/Standard_review/Isdetails?ID=MjM3NzY%3D

[28] ASTM C 1202-12: Standard Test Method for Electrical Indication of Concrete's Ability to Resist Chloride Ion Penetration[1], 2012. [Online]. Available: https://salmanco.com/wp-content/uploads/2017/06/ASTM-c-1202.pdf

[29] BIS: 516 (Part 5/Sec 2): 2021, Hardened Concrete-Methods of Test Part 5 Non-Destructive Testing Section 2 Half-Cell Potentials of Uncoated Reinforcing Steel in Concrete, New Delhi: Bureau of Indian Standards, 2021. [Online]. Available: https://www.services.bis.gov.in/php/BIS_2.0/bisconnect/standard_review/Standard_review/Isdetails?ID=MjU3OTk%3D

[30] Aditi A. Mhamal, and P.P. Savoikar, "Use of Marble and Granite Dust Waste as Partial Replacement of Fine Aggregates in Concrete," *IOP Conference Series: Earth and Environmental Science*, vol. 1130, no. 1, pp. 1-10, 2023. [CrossRef] [Google Scholar] [Publisher Link]

[31] Malkit Singh et al., "Recycling of Waste Bagasse Ash in Concrete for Sustainable Construction," *Asian Journal of Civil Engineering*, vol. 22, pp. 831-842, 2021. [CrossRef] [Google Scholar] [Publisher Link]

[32] Yash Agrawal et al., "Valorization of Granite Production Dust in Development of Rich and Lean Cement Mortar," *Journal of Material Cycles and Waste Management*, vol. 23, pp. 686–698, 2021. [CrossRef] [Google Scholar] [Publisher Link]

[33] Yogitha Bayapureddy et al., "Sugarcane Bagasse Ash as a Supplementary Cementitious Material in Cement Composites: Strength, Durability, and Microstructural Analysis," *Journal of the Korean Ceramic Society*, vol. 57, pp. 513–519, 2020. [CrossRef] [Google Scholar] [Publisher Link]

[34] Rajat Saxena et al., "Influence of Granite Waste on Mechanical and Durability Properties of Fly Ash-Based Geopolymer Concrete," *Environment, Development and Sustainability*, vol. 23, pp. 17810–17834, 2021. [CrossRef] [Google Scholar] [Publisher Link]

[35] Muhammad Nadeem et al., "Improved Water Retention and Positive Behavior of Silica Based Geopolymer Utilizing Granite Powder," *Silicon*, vol. 14, pp. 2337–2349, 2022. [CrossRef] [Google Scholar] [Publisher Link]

[36] T. Bakharev, "Geopolymeric Materials Prepared Using Class F Fly Ash and Elevated Temperature Curing," *Cement and Concrete Research*, vol. 35, no. 6, pp. 1224–1232, 2005. [CrossRef] [Google Scholar] [Publisher Link]

[37] K.I. Syed Ahmed Kabeer, and Ashok Kumar Vyas, "Utilization of Marble Powder as Fine Aggregate in Mortar Mixes," *Construction and Building Materials*, vol. 165, pp. 321–332, 2018. [CrossRef] [Google Scholar] [Publisher Link]